International Journal of Pharmaceutics 421 (2011) 310–320

Contents lists available at SciVerse ScienceDirect

International Journal of Pharmaceutics

journal homepage: www.elsevier.com/locate/ijpharm

Pharmaceutical nanotechnology

Controlled green tea polyphenols release from electrospun PCL/MWCNTs composite nanofibers

Shijun Shao[a,b], Long Li[a], Guang Yang[a], Jingrong Li[b], Chao Luo[b], Tao Gong[a], Shaobing Zhou[a,b,*]

[a] School of Materials Science and Engineering, Key Laboratory of Advanced Technologies of Material, Minister of Education, Southwest Jiaotong University, Chengdu 610031, Sichuan, PR China

[b] School of Life Science and Engineering, Southwest Jiaotong University, Chengdu 610031, Sichuan, PR China

ARTICLE INFO

Article history:
Received 28 July 2011
Received in revised form 3 September 2011
Accepted 23 September 2011
Available online 1 October 2011

Keywords:
Electrospinning
Biodegradable
Nanofibers
Controlled release

ABSTRACT

Poly(ε-caprolactone)/multi-walled carbon nanotubes (PCL/MWCNTs) composite nanofibers with various content of green tea polyphenols (GTP) were successfully fabricated via an electrospinning technology to maintain the chemical structural stability of GTP. The non-covalent interaction between MWCNTs and GTP was measured by UV–vis spectrophotometer and FT-IR. The topographical features of the nanofibers were characterized by scanning electron microscopy (SEM). The dispersibility of MWCNTs and the distribution of GTP in nanofibers were observed by transmission electron microscopy (TEM) and laser scanning confocal microscope (LSCM), respectively. *In vitro* degradation was also characterized in terms of the morphological change and the mass loss of the nanofiber meshes. *In vitro* GTP release behavior was investigated in phosphate-buffered solution (PBS) at 37 °C. Alamar blue assays were performed to estimate the cytotoxicity of the nanofibers with normal osteoblast cells and the antiproliferative effects to A549 and Hep G2 tumor cells. The results exhibited that the GTP-loaded composite nanofibers possessed a significant inhibition effect to tumor cells. Therefore, GTP, as a multifunctional drug, encapsulated into polymer composite nanofibers, must have broad application prospects in cancer therapy.

1. Introduction

Today cancer remains a serious threat to the human healthy and is a leading cause of death although we have got great accomplishment in medical science. However, traditional anticancer drug formulations have some shortcomings, e.g. short half-life in the human body, great side-effect to body and low therapeutic efficacy to solid tumors. Therefore, there have been numerous researches in order to develop more effective release systems to improve therapeutic efficacy against cancer (El-Aneed, 2004). Among these, polymeric drug controlled release system as a novel and effective method has been studied widely, and some results displayed that it has great potential in improving therapeutic efficacy, reducing toxicity and enhancing compliance of the patients by delivering drugs at a controlled rate over a period of time (Langer, 1998; Kenawy et al., 2002).

Green tea polyphenols (GTP) account for about 10% of the dry weight of green tea, which have many functions to body such as potent antioxidative activities, anti-inflammatory effects and cancer-preventive agents. Compared with other anticancer drugs, GTP exhibit little side-effect to body, but the instability (easily oxidized) limited their applications. It includes (−)-epigallocatechin-3-gallate (EGCG), (−)-epigallocatechin (EGC), (−)-epicatechin-3-gallate (ECG) and (−)-epicatechin (EC). Of these, EGCG accounts for >40% of the total (Salah et al., 1995). As a major constituent of GTP, EGCG has received a great deal of attention in previous studies and some authors even single out EGCG as the active anti-cancer component (Yoshigazawa et al., 1987; Jankun et al., 1997). The anticarcinogenic activities have been established in various organs, such as lung, skin, esophagus, duodenum, liver and stomach (Okabe et al., 1993; Stoner and Mukhtar, 1995; Blot et al., 1996; Yang et al., 1998; Leone et al., 2003).

In the study, GTP, as a model drug, was encapsulated into biodegradable polymer nanofibers by an electrospinning process to impart controlled release function and a longer stability of chemical structure of GTP. To date, there has been increasing interest in polymer nanofibers for biomedical applications, which can be fabricated by phase separation (Yang et al., 2004), template synthesis (Feng et al., 2002), self-assembly (Whitesides and Grzybowski, 2002) and electrospinning (Sill and von Recum, 2008; Agarwal et al., 2008; Puppi et al., 2010). Among these, electrospinning technology

* Corresponding author at: School of Materials Science and Engineering, Key Laboratory of Advanced Technologies of Material, Minister of Education, Southwest Jiaotong University, Chengdu 610031, Sichuan, PR China.
Tel.: +86 28 87634068; fax: +86 28 87634649.
E-mail addresses: shaobingzhou@swjtu.cn, shaobingzhou@hotmail.com (S. Zhou).

0378-5173/$ – see front matter © 2011 Elsevier B.V. All rights reserved.
doi:10.1016/j.ijpharm.2011.09.033

has been gaining increasing importance for applications in tissue engineering and drug delivery mainly due to the structural similarity to the extracellular matrix of biological tissues. Furthermore, *in vitro* studies have shown that the high surface area to volume ratio as well as the high and interconnected porosity of electrospun meshes can enhance cell adhesion, proliferation, drug loading and mass transfer properties (Li et al., 2003; Bhattarai et al., 2004).

Compared with purely polymer, composite nanofiber scaffolds incorporating inorganic nanoparticles such as $CaCO_3$ (Fujihara et al., 2005), Fe_3O_4 (Zhang et al., 2009), carbon nanotube (Mazinani et al., 2009) have attracted special attention because new properties can be obtained through the combination of different materials. Multiwalled carbon nanotubes (MWCNTs), due to their extraordinary properties such as excellent mechanical, electrical and thermal properties, are one of the most promising candidates for the design of novel composite scaffolds (Shao et al., 2011). Simultaneously, previous reports suggested that MWCNTs blended with materials may be optimal for drug delivery system (Bianco et al., 2005; Im et al., 2010). Additionally, poly(ε-caprolactone) (PCL) is a semi-crystalline poly-α-hydroxy aliphatic polyester well known for its slow biodegradability, high biocompatibility, and good drug permeability (Vandamme and Legras, 1995; Jameela et al., 1997). GTP-loaded PCL/MWCNTs composite nanofibers were fabricated for the first time by the electrospining process. The properties of electrospun composite nanofibers were studied mainly from the effects of GTP and MWCNTs incorporation on nanofiber morphology, mechanics, *in vitro* degradation and *in vitro* GTP release behaviors. The cytotoxicity for normal cells and *in vitro* antitumor activity against A549 and Hep G2 cells were also evaluated.

2. Materials and methods

2.1. Materials

Poly(ε-caprolactone) (PCL, Mw ≈ 100 kDa) was synthesized by ring-opening polymerization of ε-caprolactone monomers using stannous octoate as catalyst (Zhou et al., 2003). The molecular weight and its distribution were determined by Gel Permeation Chromatography (GPC, Waters 2695 and 2414). MWCNTs with 10–20 nm outer diameter and 10–20 μm length were purchased from Chengdu Institute of Organic Chemistry, Chinese Academy of Sciences. Green tea polyphenols (GTP) was friendly donated by Biomaterials Engineering Research Center, Sichuan University (China). Maleic anhydride and β-cyclodextrin were purchased from Kelong Chemical Reagent Company (Chengdu, China). Osteoblasts (OB) from neonatal rat's mandibular belonged to normal cell line and they were passaged to the third generation just before our experiments. The tumor cells A549 and Hep G2 were purchased from Sichuan University (China), which belonged to human lung adenocarcinoma epithelial cell line and human liver carcinoma cell line, respectively.

2.2. Preparation of the electrospun suspensions

Firstly, the raw MWCNTs were functionalized by grafting maleic anhydride (MA) on their surface through a free radical reaction and later covalently modified by β-cyclodextrin (β-CD) through an esterification reaction. Secondly, the functionalized MWCNTs were added into GTP solution of dimethyl formamide (DMF) with ultra-sonication for 30 min and then stirred continuously for about 2 h at room temperature. At the same time, PCL was dissolved in CH_2Cl_2 at room temperature. Thus, the composite PCL/MWCNTs suspensions with various content of GTP were obtained by droping GTP-adsorbed MWCNTs suspensions to PCL solutions (the volume ratio of DMF to CH_2Cl_2 was 1:1). Finally, the suspensions were ultra-sonicated for another 1 h and then stirred continuously for 24 h before electrospinning. Herein, the concentration of PCL in mixed solvent was 15 wt%, the content of MWCNTs was 3 wt% to PCL, the content of GTP was 0%, 5% and 10% (weight ratio of GTP to PCL and MWCNTs), respectively.

2.3. Electrospinning

The electrospinning process was performed as our previous reports (Zhou et al., 2008; Shao et al., 2011). In brief, the electrospun suspensions obtained above were added via a 5 mL syringe attached to a circular shaped metal capillary through a polyethylene catheter (1.5 m). The circular orifice of the capillary has an inner diameter of 0.65 mm. A plate electrode is located about 20 cm from the collecting drum. The flow rate of the suspensions was controlled within 0.8–1.2 mL/h to maintain a steady flow from the capillary outlet. The applied voltage was controlled at about 21 kV. The nanofiber meshes with various content of GTP were fabricated, dried under vacuum at room temperature for 3 days to completely remove solvent residue, stored at 4 °C. Herein, the so-called names NCF-0, NCF-5 and NCF-10 corresponded to pure PCL nanofiber meshes with GTP content of 0%, 5% and 10%, respectively, whereas CF-0, CF-5 and CF-10 stood for PCL/MWCNTs composite nanofiber meshes with GTP content of 0%, 5% and 10%, respectively.

2.4. Characterization of the composite nanofibers

2.4.1. UV–vis spectrophotometer

GTP, MWCNTs and GTP-adsorbed MWCNTs samples were characterized by UV–vis spectrophotometer (UV-2550, Shimadzu, Japan). They were prepared as follows. Firstly, an appropriate amount of GTP was fully dissolved in DMF. Secondly, small amount of MWCNTs was dispersed in DMF through ultra-sonication for about 2 h. Finally, small amount of MWCNTs was added into GTP solution, ultra-sonication for 2 h and then centrifuged to remove the excess GTP, and the resultant GTP-adsorbed MWCNTs were dispersed in DMF again through ultra-sonication for about 2 h.

2.4.2. Fourier transform infrared spectroscopy (FT-IR)

GTP, MWCNTs and MWCNTs/GTP were also characterized by Fourier transform infrared spectroscopy (FT-IR, Nicolet 5700). KBr tablets were prepared by grinding these samples with KBr and compressing the whole into a tablet at about 10 MPa.

2.4.3. Scanning electron microscopy (SEM)

The electrospun nanofiber meshes were gold-coated using sputter coating to observe the surface topographies by SEM (FEI, Quanta 200, Philips, Netherlands). The electron accelerating voltage for SEM was 20.0 kV. Micrographs from the SEM analysis were digitized and analyzed with Image Tool 2.0 to determine the average diameter of the nanofiber produced.

2.4.4. Transmission electron microscopy (TEM)

The dispersion of MWCNTs embedded in the composite PCL/MWCNTs nanofiber was observed by TEM (Hitachi H-700H) at the electron acceleration voltage of 150 kV. The sample was prepared by electrospinning PCL/MWCNTs nanofibers onto copper grids directly for about 10 s and then dried under vacuum over 24 h to remove residual solvent completely.

2.4.5. Water contact angle

The contact angle was measured using a sessile drop method at room temperature with the contact angle equipment (DSA 100, KRUSS, Germany). CA values of the right side and the left side of the distilled water droplet are both measured, and an average value is

used. All the CA data were an average of five measurements on different locations of the surface.

2.4.6. Laser scanning confocal microscope (LSCM)

The dispersion of MWCNTs embedded in the composite PCL/MWCNTs nanofibers was observed by LSCM (OLS3000). The distribution of GTP in PCL/MWCNTs (PCL) nanofibers was observed by LSCM (TCS SP2, Leica). The samples were prepared by electrospinning nanofibers onto coverslips directly for 20 s and then dried under vacuum immediately over 24 h to remove residual solvent completely.

2.4.7. Stress–strain measurements

The stress–strain analysis was performed using a universal test machine (Instron 5567, Instron Co., Massachusetts) at room temperature. The samples were trimmed into dog-bone shape specimens with the dimensions of 75 mm × 4 mm and the gauge length of 25 mm. The mean thickness was 0.18 ± 0.01 mm, and the distance between the gripping points is 30 mm. The mechanical testing was conducted with the grips moving at a stretch speed of 5 mm/min and a load cell of 5 N. The data acquisition ratio was set to 20.0 Hz. The reported data of tensile strength and elongation represent the average results of five tests.

2.5. In vitro degradation

The degradation of electrospun nanofiber meshes were performed as described previously (Peng et al., 2008). Briefly, the dried electrospun nanofiber meshes were cut into small square pieces. Each cut specimen was exactly measured for initial weight (~30 mg) and immersed in 30 mL of phosphate buffered saline (PBS, pH 7.4) in test tubes. The tubes were kept in a thermo-stated shaking air bath that was maintained at 37 °C and 120 cycles/min. Every two weeks, triplicate specimens for each nanofiber mesh were retrieved from the tubes, rinsed several times with distilled water to remove residual buffer salts, and dried to constant weight in a vacuum desiccator. The morphology was observed with SEM as described previously. The mass loss was determined gravimetrically by comparing the dry weight remaining at a predesigned time with the initial weight.

2.6. In vitro GTP release

The cumulative GTP release was investigated as incubation time for NCF-5, NCF-10, CF-5 and CF-10 nanofiber meshes. The GTP-loaded PCL/MWCNTs (PCL) nanofiber meshes (~50 mg) were incubated in 50 mL PBS in the same air bath as mentioned in degradation test. At preset interval, 1 mL of release medium was collected and 1 mL fresh PBS was added back. The GTP concentration was measured by UV–vis spectrophotometer at wavelength of 270 nm. These experiments were done in triplicate.

2.7. Cell culture in vitro

First of all, the PCL and PCL/MWCNTs nanofiber meshes with various content of GTP were cut into small round flakes with average diameter of nearly 12 mm, and then sterilized through immersion in ethanol (75%) for 2 h. After staying in sterilized PBS overnight, they can be used for cell assay. Osteoblasts were grown in α-modified essential medium (α-MEM) (HyClone, USA) with 10% fetal bovine serum (FBS). They were inoculated on the various nanofiber meshes and tissue culture plate (control) with a density of 1×10^4 cells/well in 24-well tissue culture plates (sigma Aldrich) and maintained at 37 °C in a humidified incubator with 5% CO_2. Similarly, the tumor cells (A549, Hep G2) were grown in RPMI medium 1640 (Gibcos) with 10% FBS. And followed process was similar with osteoblasts.

The proliferation viability of obsteoblast, A549 and Hep G2 was determined by means of the Alamar blue assay as specified by the manufacturer (Biosource, Nivelles, Belgium), a simple, non-toxic assay. They were indicated by measuring the reduction of resazurin to resorufin as indicator of metabolic state of cells (O'Brien et al., 2000). Cellular growth causes the reduction–oxidation indicator to change from oxidized (non-fluorescent, blue) to reduced (fluorescent, red) form. At predesigned time points, medium was carefully removed and 200 μL Alamar blue solution (10% Alamar blue, 80% media 199 (Gibcos) and 10% FBS; v/v) were added to each well and incubated for further 3 h at 37 °C. Wells without cells were used as the blank controls. Then the reduced Alamar blue was pipetted into 96-well plate (Sigma) and read at 570 (excitation)/600 (emission) in a ELISA microplate reader (Molecular Devices, Sunnyvale, CA). Results are the mean ± standard deviation of three experiments performed in triplicate.

In order to be observed by fluorescence microscopy (DMIL, Leica, Germany), the osteoblast, A549 and Hep G2 cells grown on nanofiber meshes at the 2nd and 3rd day were fixed by 2.5% glutaraldehyde for 2 h and then stained by 2-(4-amidinophenyl)-6-indolecarbamidine dihydrochloride (DAPI) (Sigma America) for about 5 min.

Additionally, the specific morphology of osteoblast, A549 and Hep G2 cells grown on the surface of nanofiber meshes was evaluated by SEM (FEI, Quanta 200, Philips, Netherlands). Firstly, they were washed twice with PBS and then fixed with 2.5% glutaraldehyde. After that, the samples were rinsed with PBS for 30 min, dehydrated through a series of graded alcohol solutions and then air-dried overnight. Finally, the dry cellular constructs were sputter coated with palladium and observed under the SEM at an accelerating voltage of 20.0 kV.

2.8. Statistics

Experiments were performed with triplicate specimens and results were reported as mean ± standard deviation. Single factorial analysis of variance (ANOVA) was performed to determine statistical significance of the data.

3. Results and discussion

3.1. Characterization of the GTP-adsorbed MWCNTs

As depicted above, the main component of green tea polyphenols (GTP) is (−)-epigallocatechin-3-gallate (EGCG), and its molecular structure is displayed in Fig. 1a. As well known, phenol is unstable, and can be easily oxidized. Herein, we encapsulated GTP into polymer matrix by electrospinning process to maintain the stability of the chemical structure. Using GTP, MWCNTs were dispersed in water through sonication, and the suspension in water was very stable, which was in good agreement with reported previously (Chen et al., 2010). The reason may be that GTP would have non-covalent interaction through π–π stacking between graphite lattice of nanotubes and the phenolic hydroxyl groups of GTP (Chen et al., 2010). The raw MWCNTs were firstly functionalized by grafting maleic anhydride (MA) on their surface through a free radical reaction and later covalently modified by β-cyclodextrin (β-CD) through an esterification reaction to improve their biocompatibility. β-Cyclodextrin was a ringed amphiphilic compounds, and the internal ring was more hydrophobic compared to the external ring. When hydrophilic and hydrophobic groups emerged simultaneously, the hydrophobic groups such as aromatic group of GTP were easier to be adsorbed by the hydrophobic cavity of β-cyclodextrin.

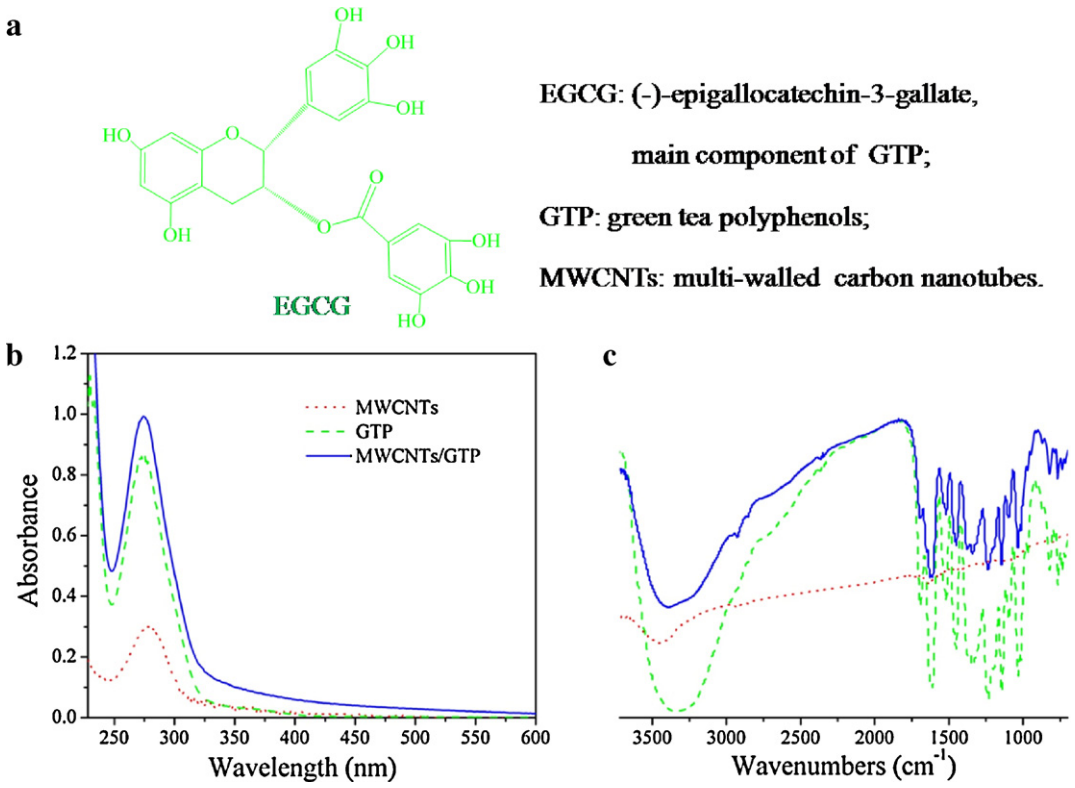

Fig. 1. Molecular structure of EGCG, main component of GTP (a), UV–vis absorption spectra (b) and FT-IR spectra (c) of MWCNTs (red), GTP (green) and GTP-absorbed MWCNTs (blue). (For interpretation of the references to color in this figure legend, the reader is referred to the web version of the article.)

In order to precisely study the relationship of GTP and MWCNTs, the functionalized MWCNTs, GTP and their composites MWCNTs/GTP were characterized by UV–visible spectrophotometer (Fig. 1b). The results showed that the characteristic absorption spectra of MWCNTS/GTP were superposition of MWCNTs and GTP basically. This indicated that GTP was adhered to the MWCNTs surface through a non-covalent interaction. In order to further define the interaction, they were also characterized with FT-IR (Fig. 1c). The characteristic absorption peak of MWCNTs on 1735 cm^{-1} was formed by ester bonds between β-cyclodextrin and maleic anhydride grafted on MWCNTs. Additionally, the infrared characteristic absorption spectra of MWCNTs/GTP was comprised by nearly all the infrared characteristic absorption peaks of GTP (3345, 1609, 1451, 1142 cm^{-1}) and MWCNTs (2923, 2852, 1629, 1654 cm^{-1}), and even β-cyclodextrin (1236 cm^{-1}) just like the UV characteristic absorption spectra. This implied that GTP was adsorbed to the MWCNTs through a non-covalent interaction once again with a negligible effect on MWCNTs and GTP vibration modes.

3.2. Characterization of GTP-loaded electrospun PCL/MWCNTs composite nanofibers

On the basis of our previous research (Shao et al., 2011), the weight ratio of MWCNTs in biodegradable polymer electrospun nanofiber mesh was 3% due to the best mechanical properties and the electrical percolation threshold. Thus, we still selected the content of MWCNTs in PCL/MWCNTs nanofibers as 3%. In Fig. 2a, the SEM images of the resultant nanofiber meshes show the effects of MWCNTs and various contents of GTP on nanofiber topographic features. It can be preliminary observed that all the nanofibers were smooth in appearance without bead-like structure. It also indicated that MWCNTs were embedded well and GTP distributed uniformly in PCL fibers. The fiber diameter was decreased with the addition of MWCNTs into polymer matrix. Additionally, from the fiber diameter distributions (Fig. 2b) we can find that the average diameter of fibers with MWCNTs was smaller than those without MWCNTs due to an increase in electric conductivity. However, with the increasing content of GTP in nanofibers the average diameter also increased gradually. The reason is mainly that the viscosity of electrospun suspensions increased and electric conductivity decreased with the increasing content of GTP.

GTP acted as a kind of surfactant actually to improve the dispersion of MWCNTs by the means of the adsorption onto surface of the hydrophobic MWCNTs. In line with the smooth surface, in many regions of the electrospun composite nanofibers the embedded MWCNTs appeared to be well-oriented along the fiber axis (Fig. 3a). Arrow direction is MWCNTs. Furthermore, TEM photo of CF-0 revealed that the MWCNTs were embedded within electrospun PCL/MWCNTs composite nanofibers (Fig. 3b). These results further proved that MWCNTs dispersed well and aligned in composite nanofibers. Fig. 3c and d shows the typical LSCM images of GTP encapsulated in PCL and PCL/MWCNTs nanofibers. From the images, we can observe that the nanofibers emitted green light due to autofluorescence of tea polyphenol, suggesting that the drug was successfully loaded in PCL matrix. The green light was distributed uniformly along these nanofibers, indicating that GTP was dispersed very uniformly in fibers. However, the fluorescence intensity of NCF-5 was slightly higher than CF-5, which illustrated that a large quantity of GTP adsorbed on surface of MWCNTs through non-covalent interactions in PCL/MWCNTs nanofibers and thus the content of GTP on the surface of nanofibers was decreased.

The stress–strain curves and mechanical properties for various PCL/MWCNTs nanofiber meshes were presented in Fig. 4. It can be seen clearly that young' modulus and maximum tensile strain were greatly improved due to the reinforcement of MWCNTs, while the elongation at break emerged an obvious reduction with the addition of MWCNTs in PCL matrix. The young' modulus,

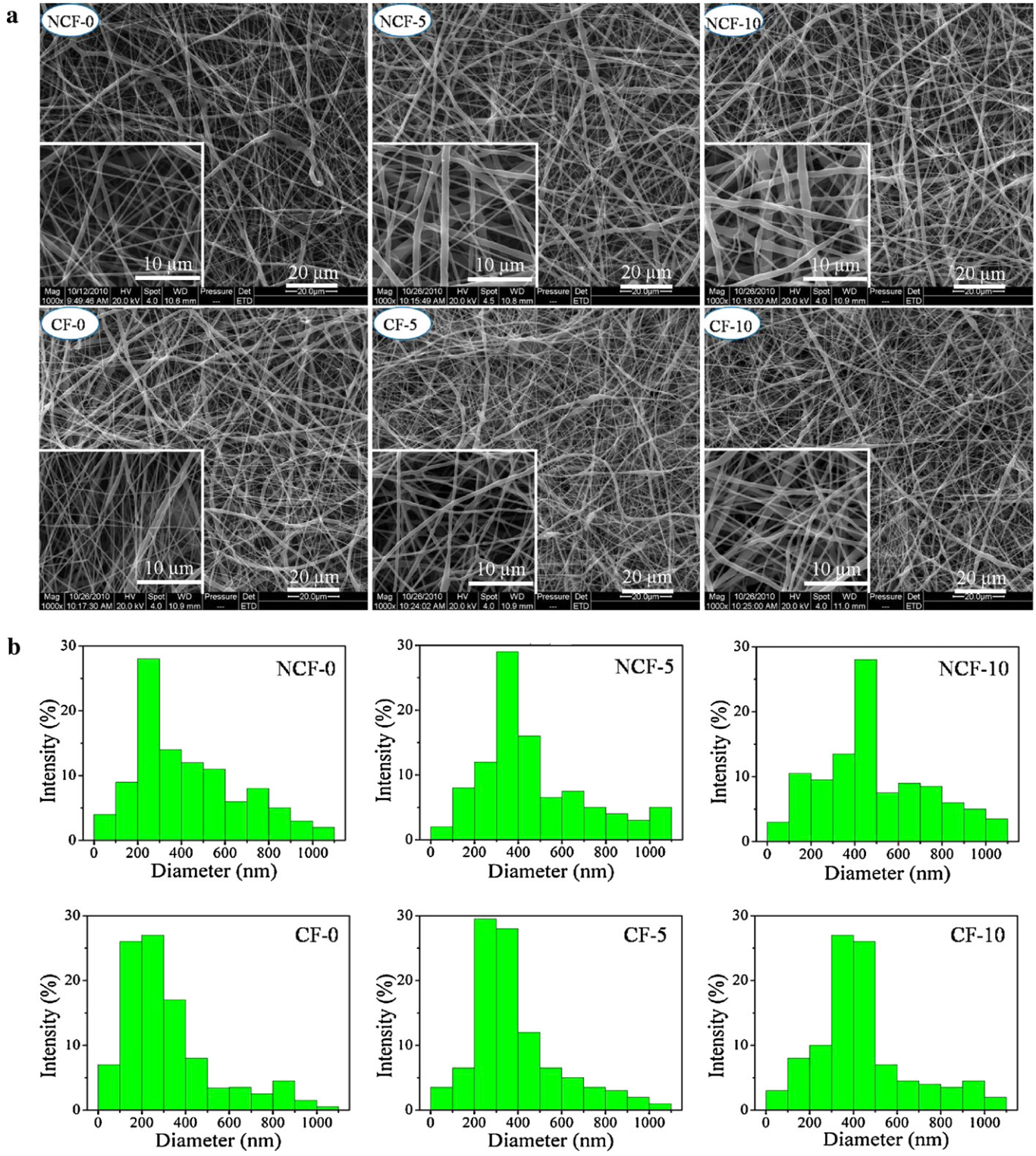

Fig. 2. Selected SEM images of electrospun nanofiber meshes without or with MWCNTs for NCF-0, NCF-5, NCF-10, CF-0, CF-5, CF-10 and their diameter distribution histograms.

maximum tensile strength and elongation at break of nanofibers showed gradually reduction with the increasing content of GTP. The young' modulus increased from 8.5 MPa for NCF-0 to 18.0 MPa for CF-0 and decreased to 5.3 MPa for NCF-10. The maximum tensile strength represented a significant improvement from 7.0 MPa for NCF-0 to 9.6 MPa for CF-0 and a reduction to 3.5 MPa for NCF-10. The elongation at break decreased from 434.6% for NCF-0 to 129.3% for CF-10.

The dispersion of MWCNTs and GTP in the polymer matrix were the most important factors in determining the mechanical properties of the PCL/MWCNTs composite nanofibers. As described above (Fig. 3), MWCNTs were well aligned along the PCL nanofiber axis, and thus mechanical properties of PCL/MWCNTs composite nanofibers increased compared with pure PCL nanofibers. It has been documented that the addition of low molecular drug had a "plasticizing" effect to fibers. Therefore, the mechanical properties

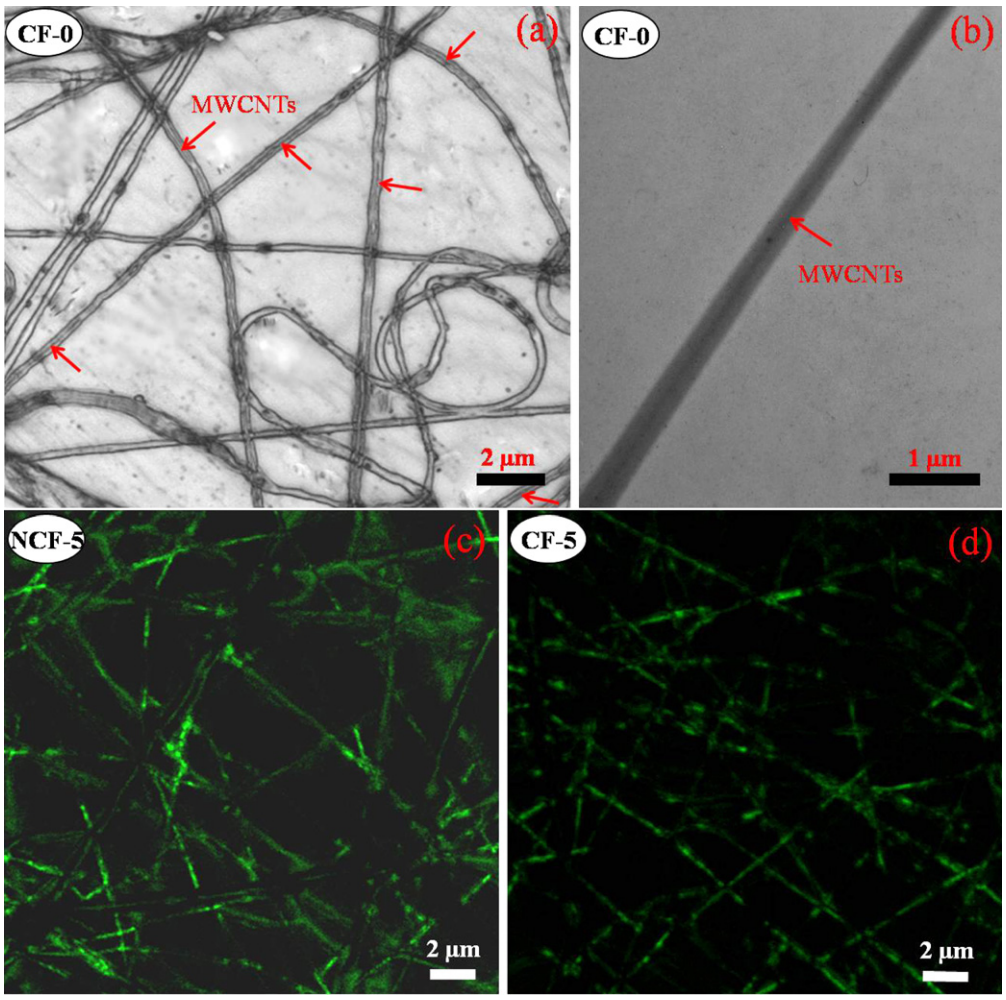

Fig. 3. Typical laser scanning confocal microscope (a) and TEM images (b) of electrospun PCL/WMCNTs composite nanofiber for CF-0; fluorescence laser scanning confocal microscope images of electrospun nanofibers without or with MWCNTs for NCF-5 (c), CF-5 (d).

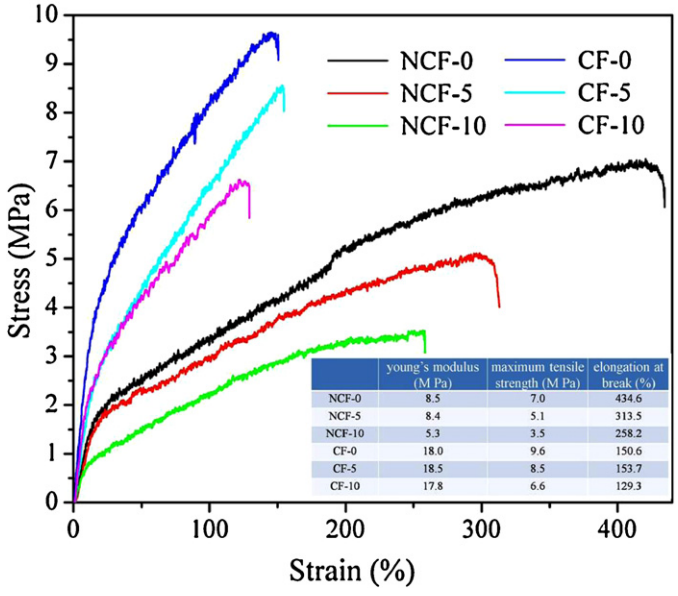

Fig. 4. Mechanical properties of NCF-0, NCF-5, NCF-10, CF-0, CF-5 and CF-10 nanofiber meshes.

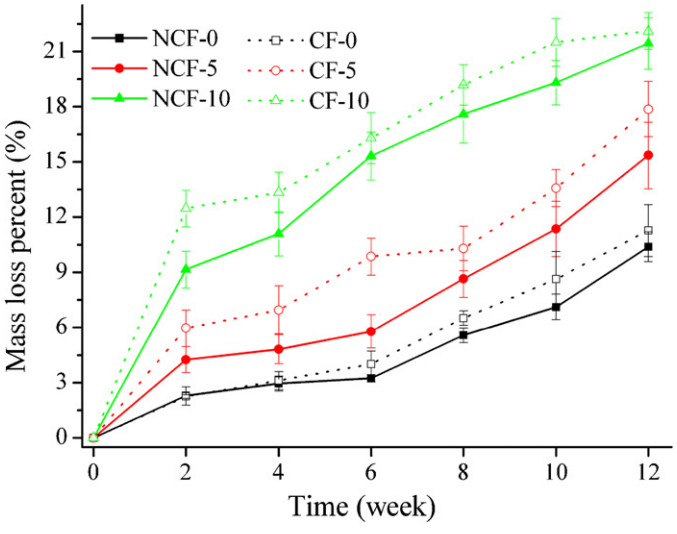

Fig. 5. The mass loss percentages of NCF-0, NCF-5, NCF-10, CF-0, CF-5 and CF-10 nanofiber meshes incubated in PBS at 37 °C.

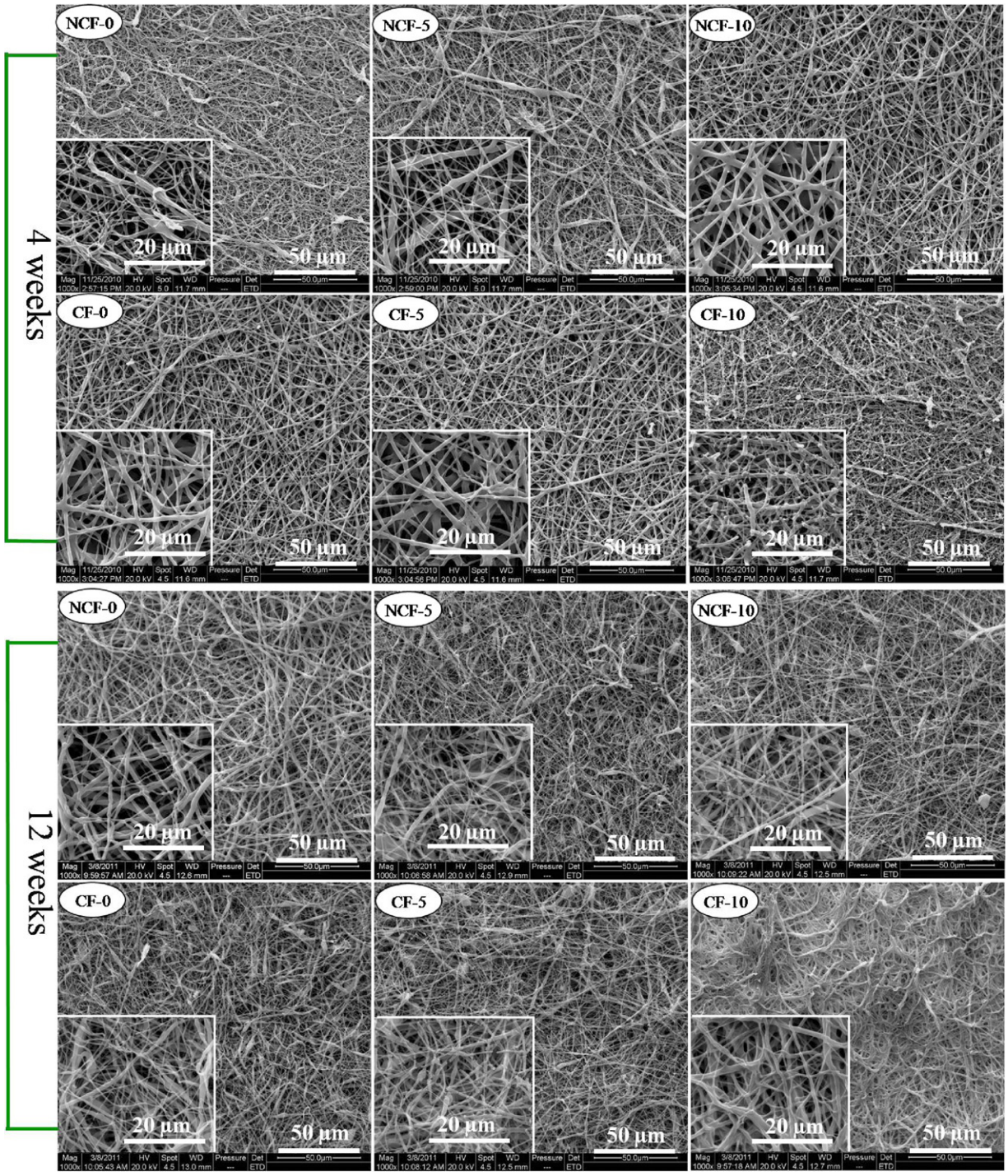

Fig. 6. Typical SEM images of NCF-0, NCF-5, NCF-10, CF-0, CF-5 and CF-10 nanofiber meshes after 4 and 12 weeks degradation in PBS at 37 °C.

of the composite nanofibers decreased with the increasing content of GTP. Furthermore, more enhancement for young's modulus was observed compared to tensile strength, which indicated that the reinforcement of MWCNTs was more prominent in the initial tensile region than the post-yield region. Additionally, the interaction between MWCNTs and polymer also affected the mechanical properties. For example, Ko et al. thought that MWCNTs hindered the crazing extension of fibers because of the alignment of MWCNTs in the crazing area and the slippage consumed extra energy (Ye et al., 2004).

3.3. In vitro degradation

The gravimetric evaluation of electrospun nanofibers during incubation was summarized in Fig. 5. The mass loss of the nanofibers occurred more rapidly over the incubation time with increased the content of GTP. Moreover, PCL/MWCNTs composite nanofibers also exhibited a little faster degradation than pure PCL nanofibers with same weight ratio of GTP.

As reported previously (Peng et al., 2008, 2009), the electrospun nanofibers with tinier diameter degraded faster due to larger

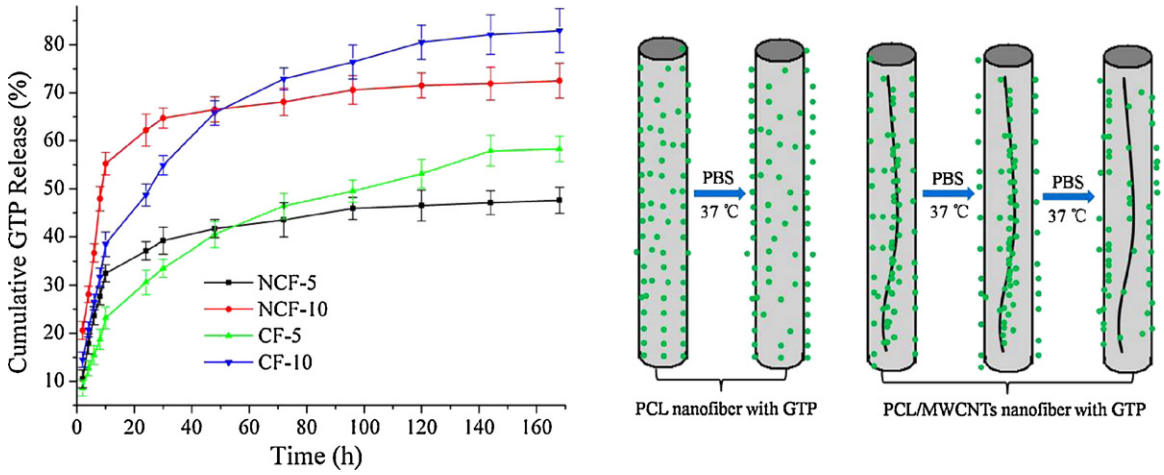

Fig. 7. *In vitro* GTP release profiles from NCF-5, NCF-10, CF-5 and CF-10 nanofiber meshes incubated in PBS at 37 °C (a); the schematic diagram of GTP controlled release from PCL and PCL/MWCNTs nanofibers (b).

specific surface when other conditions were completely same. Herein, the diameter of composite PCL/MWCNTs fibers was much smaller than pure PCL fibers, and the diameter of nanofibers gradually increased with addition of GTP. On the other hand, NCF-0 with water contact angle (~121.5°) was hydrophobic because of the nature of PCL, while the angle of CF-0 was 115.2°, suggesting that the hydrophobicity of the nanofibers was improved in the presence of the hydrophilic β-cyclodextrin functionalized MWCNTs and GTP.

The morphologies of NCF-0, NCF-5, NCF-10, CF-0, CF-5 and CF-10 nanofiber meshes after 4 and 12 weeks degradation were shown in Fig. 6. It indicated that the electrospun fibers basically remained their fibrous structure after 4 weeks degradation. However, compared with the original structure all nanofibers meshes were swollen especially for CF-10 mesh after 12 weeks degradation. The result was also consistent with mass loss mentioned above.

3.4. *In vitro* GTP release

In vitro drug release was affected mainly by these factors: the degradation rate of the carriers, hydrophobicity of drug, the content of loading drug in matrix and drug distribution. Herein, the drug "GTP" was destined to release easily in PBS because of excellent hydrophilicity of GTP. As shown in Fig. 7a, the cumulative drug release over 80% of CF-10 mesh was highest of all. In addition, drug release rate of NCF-10 and CF-10 meshes were significantly faster than NCF-5 and CF-5 meshes, which can be attributed to the increasing degradation rate of matrix and the increasing content of GTP staying on the surface of NCF-10 and CF-10 with more "GTP" compared with NCF-5 and CF-5.

In addition, both NCF-5 and NCF-10 meshes without MWCNTs have more pronounced burst release in the original 2 days than that of CF-5 and CF-10 meshes with MWCNTs. The phenomenon can be explained by the schematic diagram of GTP controlled release from PCL and PCL/MWCNTs nanofibers, as shown in Fig. 7b. In the presence of MWCNTs, GTP was mainly adsorbed on the surface of MWCNTs by non-covalent interaction through π–π stacking, as discussed above. On the contrary, GTP was distributed randomly in fiber matrix without MWCNTs. Therefore, the burst release extent of NCF-5 and NCF-10 was more seriously. In summary, the *in vitro* drug release can be controlled by adjusting the content of MWCNTs in fiber matrix.

3.5. Antiproliferative effect of the GTP-loaded nanofibers

Fig. 8 displays the proliferation viability of the normal osteoblast cells and Hep G2 and A549 tumor cells cultured on NCF-0, NCF-5, NCF-10, CF-0, CF-5, CF-10 nanofiber meshes for 5 days. The osteoblast viability cultured on all samples was more than 83%,

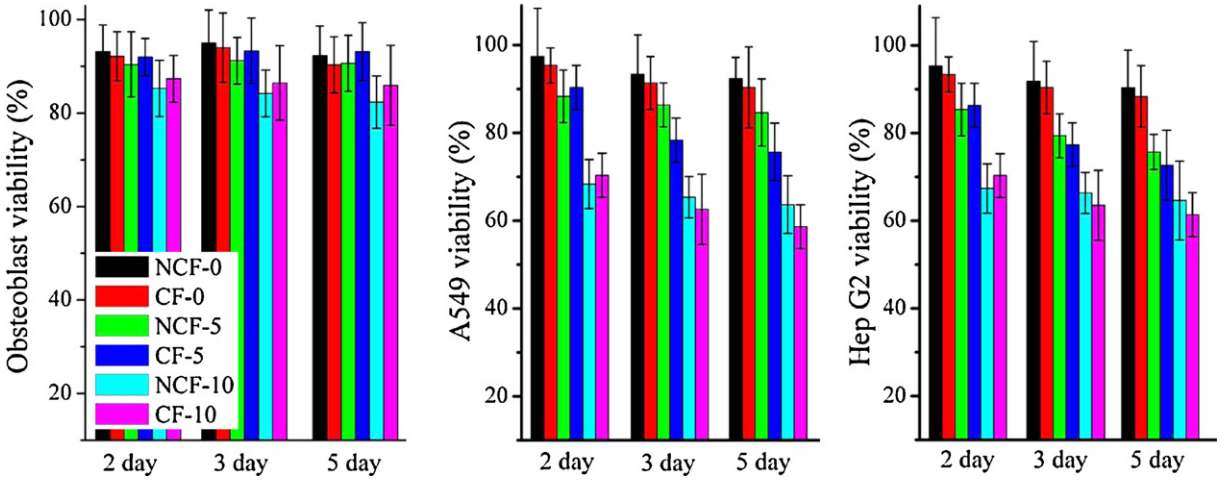

Fig. 8. Proliferation viability histograms of osteoblasts (a), A549 (b) and Hep G2 (c) cultured on NCF-0, NCF-5, NCF-10, CF-0, CF-5 and CF-10 nanofiber meshes for 2 days, 3 days and 5 days.

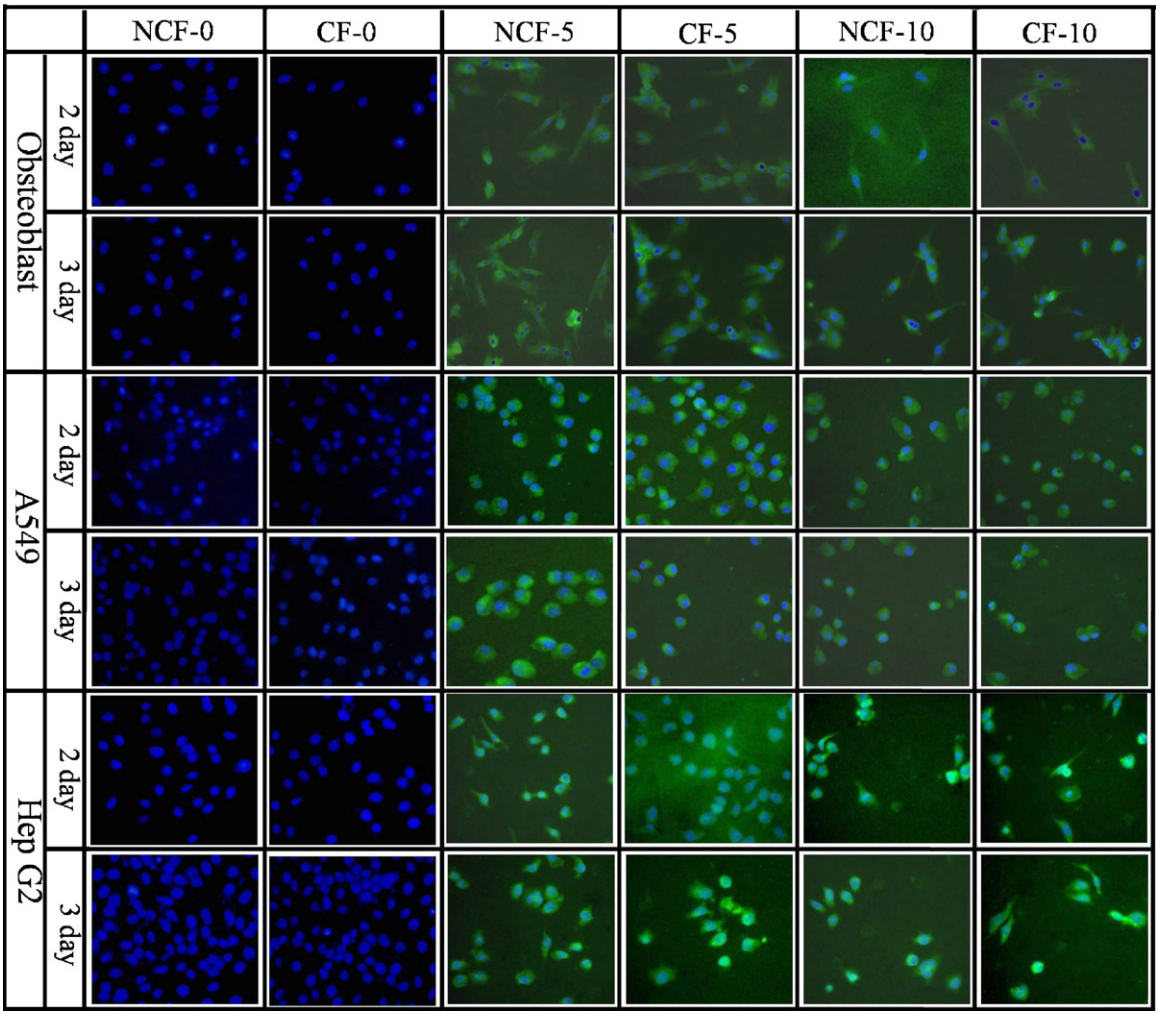

Fig. 9. Fluorescence microscope images of osteoblast, A549 and Hep G2 cultured on NCF-0, NCF-5, NCF-10, CF-0, CF-5, CF-10 nanofiber meshes for 2 and 3 days (200×).

indicating that cytotoxicity of these nanofibers were little and the electrospun nanofibers with or without GTP can meet the basic requirements for application in medicine. Besides that, the viability of osteoblast on NCF-5 (NCF-10) was slightly lower than CF-5 (CF-10) due to the serious drug burst release of NCF-5 (NCF-10). Significant statistical difference ($p < 0.05$) was detected between NCF-5 (NCF-10) and CF-5 (CF-10) at the 3rd and 5th day for cell culture.

Apart from normal cell line (osteoblast), we also studied the viability of human hepatoma cells (Hep G2) and human lung epithelial cells (A549) cultured on NCF-0, NCF-5, NCF-10, CF-0, CF-5 and CF-10 by means of Alamar blue assay. The result represented that electrospun nanofibers with GTP can inhibit the growth of tumor cells to some extent. After cell cultured for 2 days, the viability of A549 on NCF-5 (NCF-10) was slightly lower than CF-5 (CF-10) without significant statistical difference, while at the 3rd day the viability of A549 on NCF-5 (NCF-10) surpassed CF-5 (CF-10) and the divergence was more significant in the fifth day ($p < 0.05$). For Hep G2, the cell viability in other groups was almost consistent with A549, except that the inhibitory effect to Hep G2 on GTP-loaded PCL/MWCNTs composite fibers was more obvious than that to A549. The reason may be related to the difference in the total GTP release amount among these GTP-loaded nanofibers as described in GTP release section.

In order to verify the results of the Alamar blue assay, the fluorescence microscope images of osteoblasts, A549 and Hep G2 grown on all these samples after cultured for 2 and 3 days were shown in Fig. 9. The cells adhesion and morphology will also be exhaustively discussed later in our SEM section (Fig. 10). It can be seen clearly that the nanofibers substrate with GTP emitted green fluorescence due to autofluorescence of tea polyphenol, and osteoblast, A549 and Hep G2 cultured on the nanofiber meshes also showed green fluorescence due to the cellular uptake of GTP which was released from the drug-loaded nanofibers in the culture medium. Furthermore, the intensity of fluorescence inside cells turned stronger at the 3rd day than at the 2nd day. More interestingly, we can find that the intensity of fluorescence in osteoblasts was not stronger than in the tumor cells at the same period. Maybe the tumor cells preferred to phagocytose green tea polyphenols. Therefore, the drug-loaded nanofibers exhibited inhibition effect to tumor cells but not obvious effect to osteoblasts.

In order to observe the concrete morphology of osteoblasts, A549 and Hep G2 cells and their adhesions on these nanofibers, Fig. 10 displays the typical SEM photos of these cells on NCF-5 and CF-5 meshes cultured for 3 days. It can be seen that osteoblasts conglutinated and grew on NCF-5 and CF-5 meshes well especially for osteoblasts on CF-5 mesh. However, many osteoblasts on NCF-5 became spindle-like structure without visible pseudopodia at the 3rd day. By contrast, most osteoblasts adhered very well on CF-5 substrate, spreaded in all directions, and many pseudopodia grew out obviously along the unidirectional oriented nanofibers. The reason may be that the MWCNTs in nanofibers played an

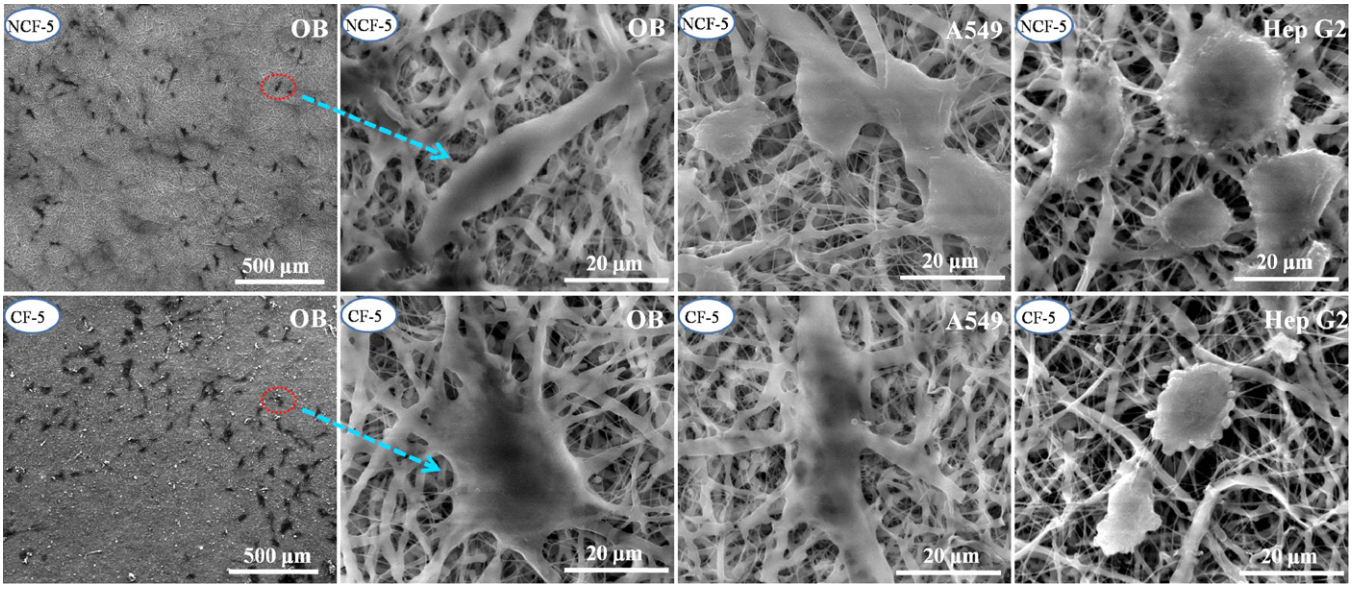

Fig. 10. Typical SEM photos of osteoblasts, A549 and Hep G2 cultured on NCF-5 and CF-5 nanofiber meshes for 3 days.

important role (Correa-Duarte et al., 2004; Abarrategi Gutierrez et al., 2008). Similarly, Webster et al. reported that carbon nanotube/poly(carbonate) urethane composites could enhance cellular functions and tissue growth by promoting the adsorption of a protein (Khang et al., 2007). The A549 represented elliptical structure and conglutinated on nanofiber meshes. However, CF-5 mesh induced apoptosis of Hep G2 cells to some extent, which was in agreement with Alamar blue analysis.

In vitro cytotoxicity evaluation of GTP showed that its inhibition effect to tumor cells was remarkable but the toxicity for normal cells was slight when the amount of GTP was small enough (Chen et al., 1998; Ahmad et al., 2000; Weisburg et al., 2004; Babich et al., 2005; Yang et al., 2006). Moreover, as mentioned above, the hydrophilicity of the electrospun nanofibers was enhanced due to the addition pf hydrophilic GTP. Thus, the affinity between cells and NCF-5, CF-5, NCF-10 and CF-10 meshes could be improved.

It has been demonstrated that green tea can inhibit the growth of several types of animal tumors, including lung cancer, esophageal cancer, hepatic carcinoma, etc. (Yang and Wang, 1993; Wang et al., 1995; Yang et al., 1997). It suggested that drinking tea was useful in prevention of angiogenesis-dependent diseases such as cancer, blindness caused by diabetes and son on. Although the cancer inhibition mechanism was not clear, Cao and Cao (1999) put forward a hypothesis that the inhibition to tumor growth and metastasis was due to that green tea can inhibit the formation of new blood vessels. Therefore, the mechanism is very important and interesting, and it is worth studying deeply in future.

4. Conclusions

We fabricated PCL/MWCNTs composite nanofibers successfully with GTP content of 0%, 5% and 10% through an electrospinning process. The average diameter of these nanofibers was affected by the addition of MWCNTs and GTP. The alignment of MWCNTs and distribution of GTP in the fibers were clearly observed from the TEM and LSCM images. The GTP can be adsorbed on the surface of MWCNTs by a non-covalent interaction through $\pi-\pi$ stacking. Both the *in vitro* degradation of the fibers and the GTP release can be controlled by supplying MWCNTs and altering GTP content. In particular, Alamar blue analysis demonstrated that the GTP-loaded composite nanofibers had low cytotoxicity for normal osteoblast cells, but high inhibition effect to tumor cells especially to Hep G2 cells. The result indicated that the GTP-loaded polymer nanofibers with little side-effect to normal body tissues possess great potential in treatment of cancers.

Acknowledgements

This work was partially supported by National Natural Science Foundation of China (30970723) and Program for New Century Excellent Talents in university, Ministry of Education of China (NCET-07-0719).

References

Ahmad, N., Gupta, S., Mukhtar, H., 2000. Green tea polyphenol epigallocatechin-3-gallate differentially modulates nuclear factor k B in cancer cells versus normal cells. Arch. Biochem. Biophys. 376, 338–346.
Abarrategi, A., Gutierrez, M., Moreno-Vicente, C., Hortiguela, M., Ramos, V., Lopez-Lacomba, J.J., Ferrer, M., Monte, F.D., 2008. Multiwall carbon nanotube scaffolds for tissue engineering purposes. Biomaterials 29, 94–102.
Agarwal, S., Wendorff, J., Greiner, A., 2008. Use of electrospinning technique for biomedical applications. Polymer 49, 5603–5621.
Blot, W.J., Chow, W.H., McLaughlin, J.K., 1996. Tea and cancer: a review of the epidemiological evidence. Eur. J. Cancer Prev. 5, 425–438.
Bhattarai, S.R., Bhattarai, N., Yi, H.K., Hwang, P.H., Cha, D., Kim., H.Y., 2004. Novel biodegradable electrospun membrane: scaffold for tissue engineering. Biomaterials 25, 2595–2602.
Babich, H., Krupka, M.E., Nissim, H., Zuckerbraun, H., 2005. Differential in vitro cytotoxicity of (−)-epicatechin gallate (ECG) to cancer and normal cells from the human oral cavity. Toxicol. In Vitro 19, 231–242.
Bianco, A., Kostarelos, K., Prato, M., 2005. Applications of carbon nanotubes in drug delivery. Curr. Opin. Chem. Biol. 9, 674–679.
Chen, Z., Schell, J., Ho, C., Chen, K., 1998. Green tea epigal-locatechin gallate shows a pronounced growth inhibitory effect on cancerous cells but not on their normal counterparts. Cancer Lett. 129, 173–179.
Cao, Y., Cao, R., 1999. Angiogenesis inhibited by drinking tea. Nature 398, 381.
Correa-Duarte, M., Wagner, N., Rojas-Chapana, J., Morsczeck, C., Thie, M., Giersig, M., 2004. Fabrication and biocompatibility of carbon nanotube-based 3D networks as scaffolds for cell seeding and growth. Nano Lett. 4, 2233–2236.
Chen, Y., Lee, Y.D., Vedala, H., Allen, B., Star, A., 2010. Exploring the chemical sensitivity of a carbon nanotube/green tea composite. Acs Nano 4, 6854–6862.
El-Aneed, A., 2004. An overview of current delivery systems in cancer gene therapy. J. Control. Release 94, 1–14.
Feng, L., Li, S.H., Li, Y.S., Li, H., Zhang, L.J., Zhai, J., Song, Y.L., Liu, B.Q., Jiang, L., Zhu, D.B., 2002. Super-hydrophobic surfaces: from natural to artificial. Adv. Mater. 14, 1857–1860.
Fujihara, K., Kotaki, M., Ramakrishna, S., 2005. Guided bone regeneration membrane made of polycaprolactone/calcium carbonate composite fibers. Biomaterials 26, 4139–4147.

Im, J., Bai, B.C., Lee, Y.S., 2010. The effect of carbon nanotubes on drug delivery in an electro-sensitive transdermal drug delivery system. Biomaterials 31, 1414–1419.
Jankun, J., Selman, S.H., Swiercz, R., Ewa, E.S., 1997. Why drinking green tea could prevent cancer. Nature 387, 561.
Jameela, S., Suma, N., Jayakrishnan, A., 1997. Protein release from poly(epsilon-caprolactone) microspheres prepared by melt encapsulation and solvent evaporation techniques: a comparative study. J. Biomater. Sci. Polym. Ed. 8, 457–466.
Kenawy, E., Bowlin, G.L., Mansfield, K., Layman, J., Simpson, D.G., Sanders, E.H., Wnek, G.E., 2002. Release of tetracycline hydrochloride from electrospun poly(ethylene-co-vinylacetate), poly(lactic acid), and a blend. J. Control. Release 81, 57–64.
Khang, D., Kim, S., Liu-Snyder, P., Palmore, G., Durbinc, S., Webster, T., 2007. Enhanced fibronectin adsorption on carbon nanotube/poly(carbonate) urethane: independent role of surface nano-roughness and associated surface energy. Biomaterials 28, 4756–4768.
Langer, R., 1998. Drug delivery and targeting. Nature 392, 5–10.
Leone, M., Zhai, D.Y., Sareth, S., Kitada, S., Reed, J.C., Pellecchia, M., 2003. Cancer prevention by tea polyphenols is linked to their direct inhibition of antiapoptotic Bcl-2-family proteins. Cancer Res. 63, 8118–8121.
Li, D., Wang, Y., Xia, Y., 2003. Electrospinning of polymeric and ceramic nanofibers as uniaxially aligned arrays. Nano Lett. 3, 1167–1171.
Mazinani, S., Ajji, A., Dubois, C., 2009. Morphology, structure and properties of conductive PS/CNT nanocomposite electrospun mat. Polymer 50, 3329–3342.
Okabe, S., Suganuma, M., Hayashi, M., Sueoka, E., Komori, A., Fujiki, H., 1993. Mechanisms of growth inhibition of human lung cancer cell line, PC-9, by tea polyphenols. Cancer Sci. 88, 639–643.
O'Brien, J., Wilson, I., Orton, T., Pognan, F., 2000. Investigation of the alamar blue (resazurin) fluorescent dye for the assessment of mammalian cell cytotoxicity. Eur. J. Biochem. 267, 5421–5426.
Peng, H., Zhou, S.B., Guo, T., Li, Y.S., Li, X.H., Wang, J.X., Weng, J., 2008. In vitro degradation and release profiles for electrospun polymeric fibers containing paracetanol. Colloids Surf. B 66, 206–212.
Peng, H.S., Zhou, S.B., Jiang, J., Guo, T., Zheng, X.T., Yu, X., 2009. Pressure-induced crystal memory effect of spider silk proteins. J. Phys. Chem. B 113, 4636–4641.
Puppi, D., Piras, A.M., Nicola, D., Dinucci, D., Chiellini, F., 2010. Poly(lactic-co-glycolic acid) electrospun fibrous meshes for the controlled release of retinoic acid. Acta Biomater. 6, 1258–1268.
Stoner, G.D., Mukhtar, H., 1995. Polyphenols as cancer chemopreventive agents. J. Cell. Biochem. 22, 169–180.
Salah, N., Miller, N.J., Paganga, G., Tijburg, L., Bolwell, G.P., Rice-Evans, C., 1995. Polyphenolic flavanols as scavengers of aqueous phase radicals and as chain-breaking antioxidants. Arch. Biochem. Biophys. 322, 339–346.
Sill, T.J., von Recum, H.A., 2008. Electrospinning: applications in drug delivery and tissue engineering. Biomaterials 29, 1989–2006.
Shao, S.J., Zhou, S.B., Li, L., Li, J.R., Luo, C., Wang, J., Wang, J.X., Li, X.H., Weng, J., 2011. Osteoblast function on electrically conductive electrospun PLA/MWCNTs nanofibers. Biomaterials 32, 2821–2833.
Vandamme, T., Legras, R., 1995. Physico-mechanical properties of poly(ε-caprolactone) for the construction of rumino-reticulum devices for grazing animals. Biomaterials 16, 1395–1400.
Wang, Z.Y., Wan, L.D., Lee, M.J., Ho, C.T., Huang, M.T., Conney, A.H., Yang, C.S., 1995. Inhibition of N-nitrosomethylbenzylamine-induced esophageal tumorigenesis in rats by green and black tea. Carcinogenesis 16, 2143–2148.
Whitesides, G.M., Grzybowski, B., 2002. Self-assembly at all scales. Science 295, 2418–2421.
Weisburg, J., Weissman, D., Sedaghat, T., Babich, H., 2004. In vitro cytotoxicity of epigallocatechin gallate and tea extracts to cancerous and normal cells from the human oral cavity. Basic Clin. Pharmacol. Toxicol. 95, 191–200.
Yoshigazawa, S., Horiuchi, T., Fujiki, H., Yoshida, T., Okuda, T., 1987. Antitumor promoting activity of (−)-epigallocatechin gallate, the main constituent of 'tannin' in green tea. Phytother. Res. 1, 44–47.
Yang, C., Wang, Z., 1993. Tea and Cancer. J. Natl. Cancer Inst. 85, 1038–1049.
Yang, G., Wang, Z., Kim, S., Liao, J., Seril, D., Chen, X., Smith, T.J., Yang, C.S., 1997. Characterization of early pulmonary hyperproliferation and tumor progression and their inhibition by black tea in a 4-(methylnitrosamino)-1-(3-pyridyl)-1-butanone-induced lung tumorigenesis model with A/J mice. Cancer Res. 57, 1889–1894.
Yang, G.Y., Liao, J., Kim, K., Yurkow, E.J., Yang, C.S., 1998. Inhibition of growth and induction of apoptosis in human cancer cell lines by tea polyphenols. Carcinogenesis 19, 611–616.
Yang, F., Murugan, R., Ramakrishna, S., Wang, X., Ma, Y.X., Wang, S., 2004. Fabrication of nano-structured porous PLLA scaffold intended for nerve tissue engineering. Biomaterials 25, 1891–1900.
Ye, H., Lam, H., Titchenal, N., Gogotsi, Y., Ko, F., 2004. Reinforcement and rupture behavior of carbon nanotubes-polymer nanofibers. Appl. Phys. Lett. 85, 1775–1777.
Yang, C., Lambert, J., Hou, Z., Ju, J., Lu, G., Hao, X., 2006. Molecular target for cancer preventive activity of tea polyphenols. Mol. Carcinog. 45, 431–535.
Zhang, D., Karki, A., Rutman, D., Young, D., Wang, A., Cocke, D., Wangc, A., Cockea, D., Hoa, T., Guo, Z.H., 2009. Electrospun polyacrylonitrile nanocomposite fibers reinforced with Fe_3O_4 nanoparticles: fabrication and property analysis. Polymer 50, 4189–4198.
Zhou, S., Deng, X., Yang, H., 2003. Biodegradable poly(ε-caprolactone)–poly(ethylene glycol) block copolymers: characterization and their use as drug carriers for a controlled delivery system. Biomaterials 24, 3563–3570.
Zhou, S., Peng, H., Yu, X., Zheng, X., Cui, W., Zhang, Z., Li, X., Wang, J., Weng, J., Jia, W., Li, F., 2008. Preparation and characterization of a novel electrospun spider silk fibroin/poly(D,L-lactide) composite fiber. J. Phys. Chem. B 112, 11209–11216.